

# Second order phase transition in the six-dimensional Ising spin glass on a field

M. Aguilar-Janita

*Complex Systems Group, Universidad Rey Juan Carlos, 28933 Móstoles, Madrid, Spain*

V. Martin-Mayor

*Departamento de Física Teórica, Universidad Complutense, 28040 Madrid, Spain and  
Instituto de Biocomputación y Física de Sistemas Complejos (BIFI), 50018 Zaragoza, Spain*

J. Moreno-Gordo

*Instituto de Biocomputación y Física de Sistemas Complejos (BIFI), 50018 Zaragoza, Spain  
Departamento de Física Teórica, Universidad de Zaragoza, 50009 Zaragoza, Spain  
Departamento de Física, Universidad de Extremadura, 06006 Badajoz, Spain and  
Instituto de Computación Científica Avanzada (ICCAEx),  
Universidad de Extremadura, 06006 Badajoz, Spain*

J.J. Ruiz-Lorenzo

*Departamento de Física, Universidad de Extremadura, 06006 Badajoz, Spain  
Instituto de Computación Científica Avanzada (ICCAEx),  
Universidad de Extremadura, 06006 Badajoz, Spain and  
Instituto de Biocomputación y Física de Sistemas Complejos (BIFI), 50018 Zaragoza, Spain  
(Dated: June 2, 2023)*

The very existence of a phase transition for spin glasses in an external magnetic field is controversial, even in high dimensions. We carry out massive simulations of the Ising spin-glass in a field, in six dimensions (which, according to classical—but not generally accepted—field-theoretical studies, is the upper critical dimension). We find a phase transition and compute the critical exponents, that are found to be compatible with their mean-field values. We also find that the replica-symmetric Hamiltonian describes the scaling of the renormalized couplings near the phase transition.

The existence of a spin-glass (SG) transition in the presence of an external magnetic field, at the so-called de Almeida-Thouless (dAT) line [1], is one of the most challenging problems in the realm of disordered systems [2–5]. The existence of the dAT line is only firmly established in the limit of infinite space dimensions,  $D \rightarrow \infty$  [2].

In order to clarify this problem, the community has tried to implement the Wilson renormalization group (RG) program [6, 7]. The starting point is the computation of the so-called upper critical-dimension  $D_u$  (the smallest  $D$  at which critical exponents take their Gaussian values). Unfortunately, this approach, extremely successful in a huge variety of problems including SG at zero field [8, 9], has not yet succeed. Replicated field-theory finds  $D_u = 6$  but fails to find, in the one-loop approximation, a fixed point stable at  $D = 6$  [10, 11]. In fact, we identify no less than five conflicting scenarios:

(i) The droplets model predicts the absence of a dAT line for any  $D < \infty$  (i.e. the so-called *lower* critical dimension is  $D_l = \infty$ ) [12–15].

(ii) A modified version of the droplets model, finds  $D_u = D_l = 6$ . In other words, a spin-glass phase transition would be possible in a field only if  $D > 6$  [16]. See also Refs. [17] and [18]. The summation of high temperature series conforms to this view [19].

(iii) A very recent field-theoretical analysis claims  $D_u = 8$  [20]. Interestingly enough, a two-loop computation does find a non-trivial stable fixed point at  $D = 6$  [21, 22], the Gaussian one being unstable. This non-trivial fixed-

point would lie in the non-perturbative region (which makes it unclear whether or not the fixed point would survive a three-loops computation).

(iv) Yet another scenario predicts a quasi-first order transition in a field [23] (this scenario was critically assessed in [24]).

(v) Large scale numerical simulations suggest the presence of a dAT line for  $D = 4$  [25], but the results are not conclusive for  $D = 3$  [26, 27].

Here, we add clarity to the debate by showing that a dAT line is present in  $D = 6$  through massive numerical simulations: our largest lattices contain  $8^6$  spins, more than twice the  $48^3$  spins in the largest system ever equilibrated in  $D = 3$  [28]. We find that the scaling behaviour of the different susceptibilities is qualitatively different from their zero field counterpart. Our computed critical exponents turn out to be compatible with their Gaussian values, which suggests  $D_u = 6$ . We also confirm the validity of two-parameter Replica Symmetric (RS) effective Hamiltonian [10] to describe the scaling of the coupling constants in the critical region, which enable us to discuss the problem of a second order phase transition versus a random first order one.

We consider the Edwards-Anderson Hamiltonian for Ising spins (i.e.  $s_{\mathbf{x}} = \pm 1$ ) on a six dimensional cubic lattice of size  $V = L^6$ , with periodic boundary conditions and nearest-neighbors interactions:

$$\mathcal{H} = - \sum_{\langle \mathbf{x}, \mathbf{y} \rangle} J_{\mathbf{x}\mathbf{y}} s_{\mathbf{x}} s_{\mathbf{y}} - h \sum_{\mathbf{x}} s_{\mathbf{x}}, \quad (1)$$

where the couplings are independent, identically distributed random variables ( $J_{\mathbf{x}\mathbf{y}} = \pm 1$  with equal probability). Hereafter, the over line  $(\overline{\dots})$  means average over the couplings, while  $\langle(\dots)\rangle$  is the thermal average carried-out for fixed couplings  $\{J_{\mathbf{x}\mathbf{y}}\}$ . A choice of couplings is named a *sample*.

*a. Field-theoretical framework.* The analysis of the RS Hamiltonian in the field theory finds three masses (replicon, anomalous and longitudinal) and their associated propagators (correlation functions) [11, 29]. In the spin glass phase, the most singular mode is the replicon. The anomalous and longitudinal modes become identical when one takes the limit for the number of replicas  $n$  going to zero. Hence the two fundamental propagators of the theory,  $G_R(\mathbf{x} - \mathbf{y})$  and  $G_A(\mathbf{x} - \mathbf{y})$ , are defined as (see App. A for more details)

$$G_R(\mathbf{x} - \mathbf{y}) = \overline{\langle s_{\mathbf{x}} s_{\mathbf{y}} \rangle^2} - 2 \overline{\langle s_{\mathbf{x}} s_{\mathbf{y}} \rangle \langle s_{\mathbf{x}} \rangle \langle s_{\mathbf{y}} \rangle} + \overline{\langle s_{\mathbf{x}} \rangle^2 \langle s_{\mathbf{y}} \rangle^2} \quad (2)$$

and

$$G_A(\mathbf{x} - \mathbf{y}) = \overline{\langle s_{\mathbf{x}} s_{\mathbf{y}} \rangle^2} - 4 \overline{\langle s_{\mathbf{x}} s_{\mathbf{y}} \rangle \langle s_{\mathbf{x}} \rangle \langle s_{\mathbf{y}} \rangle} + 3 \overline{\langle s_{\mathbf{x}} \rangle^2 \langle s_{\mathbf{y}} \rangle^2}. \quad (3)$$

Associated with each two-points correlation functions one can define a susceptibility  $\chi$  as

$$\chi_{\alpha} = \hat{G}_{\alpha}(\mathbf{0}) \quad \alpha \in \{R, A\}, \quad (4)$$

where  $\hat{G}(\mathbf{k})$  is the discrete Fourier transform of  $G(\mathbf{x})$ . In the  $h = 0$  case, it is straightforward to show that  $\chi_R = \chi_A = \chi_L$ . When  $h \neq 0$  instead, we shall find below that  $\chi_R$  becomes dominant in the spin glass phase.

In order to study the RS effective Hamiltonian, one introduces the following parameter  $\lambda$  (details in App. C)

$$\lambda = \frac{w_2}{w_1}, \quad (5)$$

where  $w_1$  and  $w_2$  are the coefficients (i.e., the exact vertices) of the static replicated Gibbs free energy [29]. These exact vertices can be expressed as

$$w_i = \frac{\omega_i}{\chi_R^3}, \quad i = 1, 2, \quad (6)$$

where  $\omega_1$  and  $\omega_2$  are the coefficients of the Helmholtz free energy (i.e., non-linear connected susceptibilities, see App. B), which as usual, is the Legendre transform of the Gibbs free energy. Both  $\omega_1$  and  $\omega_2$  can be computed as three-point connected correlation functions at zero external momentum

$$\omega_1 = \frac{1}{V} \sum_{\mathbf{x}\mathbf{y}\mathbf{z}} \overline{\langle s_{\mathbf{x}} s_{\mathbf{y}} \rangle_c \langle s_{\mathbf{y}} s_{\mathbf{z}} \rangle_c \langle s_{\mathbf{z}} s_{\mathbf{x}} \rangle_c}, \quad (7)$$

$$\omega_2 = \frac{1}{2V} \sum_{\mathbf{x}\mathbf{y}\mathbf{z}} \overline{\langle s_{\mathbf{x}} s_{\mathbf{y}} s_{\mathbf{z}} \rangle_c^2}, \quad (8)$$

where the c subindices stand for *connected* correlation functions. Hence,

$$\lambda \equiv \frac{w_2}{w_1} = \frac{\omega_2}{\omega_1}. \quad (9)$$

In addition, it is possible to show that  $\lambda$  does not renormalize, so  $\lambda = \lambda_r$ .

Furthermore,  $\lambda$  is also related with the cubic couplings  $\tilde{w}_1$  and  $\tilde{w}_2$  of the RS effective Hamiltonian because, at the lowest order in perturbation theory, we have  $\tilde{w}_i = w_i$  ( $i = 1, 2$ ). Then,  $\lambda$  signals the breaking point from a RS to Replica Symmetry Breaking scenario. For additional details see Refs. [24, 29].

Finally, let us remark that there are two different ways of taking the limits for  $\lambda(L, T)$  at  $T_c$

$$\lambda^* = \lim_{L \rightarrow \infty} \lim_{T \rightarrow T_c} \lambda(L, T), \quad \lambda(T_c^+) = \lim_{T \rightarrow T_c} \lim_{L \rightarrow \infty} \lambda(L, T). \quad (10)$$

In principle,  $\lambda^* \neq \lambda(T_c^+)$ . We are interested in  $\lambda(T_c^+)$ .

Notice that six real replicas (six independent copies of the system evolving under the same couplings) are needed to compute  $\omega_1$  and  $\omega_2$ . However, one can compute  $\omega_1$  and  $\omega_2$  in terms of three and four real-replicas estimators (see App. C). Within the framework of the RS theory [29], the values of the three and four-replicas estimators differ in general from the true values of  $\omega_1$  and  $\omega_2$  but coincide with them at the critical temperature. This gives us the opportunity to check the validity of the RS theory by computing the six, four and three-replicas estimators. [30]

Another check is the value of  $\lambda$  itself, since the replica symmetric field theory predicts a value of  $0 \leq \lambda \leq 1$  for a second order phase transition while a value of  $\lambda > 1$  would imply the presence of a peculiar type of first-order phase transition [23]. It is worth noting that  $\lambda$  controls as well the Mean-Field (MF) values of equilibrium and off-equilibrium dynamical exponents [29].

*b. Finite Size Scaling.* We want to investigate whether or not the systems undergoes a second-order phase transition in the presence of a magnetic field and, if the answer is positive, to characterize the resulting universality class. Indeed, a standard way of identifying a phase transition is computing some correlation length  $\xi$ , that is used to identify scale invariance. An appropriate definition of the second-moment correlation length in a finite lattice is [7]

$$\xi_2 = \frac{1}{2 \sin(\pi/L)} \left( \frac{\hat{G}_R(0)}{\hat{G}_R(\mathbf{k}_1)} - 1 \right)^{1/2}. \quad (11)$$

where  $\mathbf{k}_1 = (2\pi/L, 0, 0, 0, 0, 0)$  (or permutations). The scale invariance of  $\xi_2/L$  at the critical point results in

$$\frac{\xi_2}{L} = f_{\xi}(L^{\frac{1}{\nu}} t) + L^{-\omega} g_{\xi}(L^{\frac{1}{\nu}} t) + \dots \quad (12)$$

where  $\omega$  is the correction-to-scaling exponent and  $t = (T - T_c)/T_c$  is the reduced temperature. From this behaviour one expects that a plot of  $\xi_2(T)/L$  for several system sizes will show a common intersection point at  $T = T_c$ , provided that the sizes are large enough to make corrections to scaling negligible. However, previous works in lower dimensions [25, 31] did not find this

intersection. This anomalous behaviour was attributed to an abnormal behavior of the propagator at wave vector  $\mathbf{k} = \mathbf{0}$  [31], that induces strong corrections to the leading scaling-behaviour in Eq. (12). This phenomenon is illustrated through the spin-glass order parameter distribution in the App. D.

Given the aforementioned anomaly, we consider a second scale-invariant quantity, previously introduced in Ref. [25] under the name  $R_{12}$ , which is computed as a dimensionless ratio of propagators with higher momenta

$$R_{12} = \frac{\widehat{G}_R(\mathbf{k}_1)}{\widehat{G}_R(\mathbf{k}_2)}. \quad (13)$$

Here,  $\mathbf{k}_1$  and  $\mathbf{k}_2$  are the smallest nonzero momenta compatible with periodic boundary conditions, namely  $\mathbf{k}_1 = (2\pi/L, 0, 0, 0, 0, 0)$  and  $\mathbf{k}_2 = (2\pi/L, \pm 2\pi/L, 0, 0, 0, 0)$  (and permutations). Notice that  $R_{12}$  scales in the same way as  $\xi_2/L$ , see Eq. (12).

*c. Numerical results.* We have studied the model in Eq. (1) through Monte Carlo simulations on lattices  $L = 5, 6, 7$  and  $8$ , with a magnetic field set to  $h = 0.075$ . Thermalization is ensured by using the parallel tempering algorithm [32, 33], complemented with a demanding equilibration test based on Ref. [34]. In order to obtain high statistics, we have simulated 25600 samples for  $L = 5, 6, 7$  and 5120 for the largest lattice size  $L = 8$  by using multispin coding. Six statistically independent system copies of each sample, named real replicas, are simulated in order to compute without statistical bias both  $\omega_1$  and  $\omega_2$ , recall Eqs. (7) and (8). Further details about our simulations are provided in App. E.

One may question if our magnetic field  $h = 0.075$  is large enough to ensure that we are working far-enough from the  $h = 0$  endpoint of the dAT line. We answer that question by computing the replicon and anomalous susceptibilities: notice that for  $h = 0$ ,  $\chi_R = \chi_A$ . In Fig. 1 we represent  $\chi_R$  and  $\chi_A$ . Indeed, at the critical point even our smallest system  $L = 5$  has  $\chi_R(L = 5, T_c) \approx 5\chi_A(L = 5, T_c)$ , and this ratio gets larger as  $L$  grows [35], meaning that correlations extend to a much longer distance for the replicon mode than for the anomalous one, in agreement with both the MF picture and previous computations in  $D = 3$  [26] and  $D = 4$  [24].

We start by determining the value of the critical temperature at which the phase transition takes place. Eq. (12) tells us that the curves of dimensionless magnitudes such as  $\xi_2/L$  and  $R_{12}$ , when computed for different system sizes, will intersect at  $T_c(h)$ . These intersections are shown in Fig. 2 and in Table I. Corrections to scaling cause the intersection points to vary, depending on the considered pair of lattice  $(L_1, L_2)$  and the quantity under inspection,  $\xi_2/L$  or  $R_{12}$ . However, for our largest systems ( $L_1 = 7$ ,  $L_2 = 8$ ) we find compatible crossings for  $\xi_2/L$  and  $R_{12}$ . Also the  $(L_1 = 6, L_2 = 7)$  crossing for  $R_{12}$  turns out to be compatible with the results from  $(L_1 = 7, L_2 = 8)$ . Although a more accurate estimation of  $T_c$  is obtained below, the reader can already appreciate that  $T_c(h = 0.075)$  is significantly smaller than its  $h = 0$

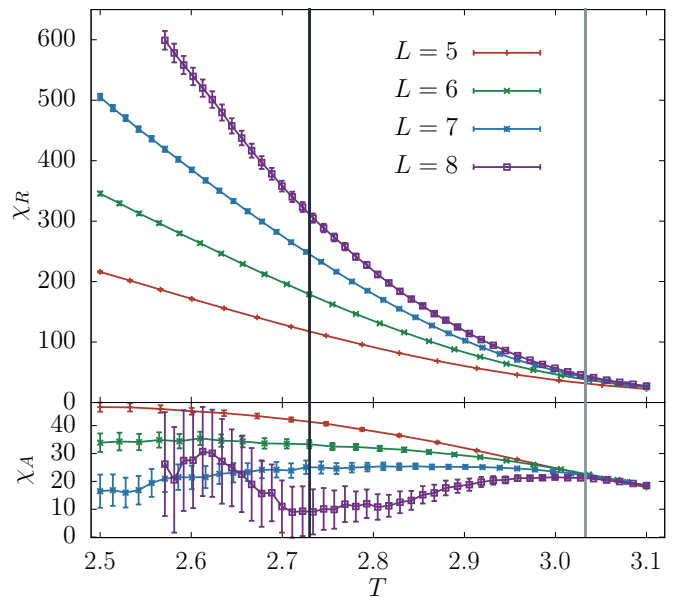


FIG. 1. Susceptibilities for the replicon  $\chi_R$  (on the **top**), Eqs. (2) and (A8), and for the anomalous mode  $\chi_A$  (on the **bottom**), Eqs. (3) and (A8), versus temperature  $T$ , as computed for our different system sizes in a magnetic field  $h = 0.075$ . For  $h = 0$  one trivially shows that  $\chi_R = \chi_A$ . Instead, for  $h = 0.075$ , we find that  $\chi_R$  rapidly grows with  $L$  at low temperatures, while  $\chi_A$  remains bounded. The different size dependence ensures that we are working far enough from the  $h = 0$  point in the dAT line. The two vertical lines are our estimates for the critical temperatures for  $h = 0.075$  (left vertical line) and for  $h = 0$  (right line).

counterpart  $T_c(h = 0) = 3.033(1)$  [36, 37] (see also App. H).

Our next step is the characterization of the universality class by computing critical exponents  $\nu$  (associated with the correlation length) and  $\eta$  (associated with the replicon susceptibility). We extract effective, size-dependent exponents by using the quotient method [38–40] (see Table II). To avoid the somewhat problematic  $\mathbf{k} = \mathbf{0}$  wave vector we compute  $\nu$  from the scaling of  $\partial R_{12}/\partial T$  (see App. G) and  $\eta$  from the susceptibility  $\mathcal{F}$ :

$$\mathcal{F} = \widehat{G}_R(\mathbf{k}_1). \quad (14)$$

The effective exponents in Table II need to be extrapolated to  $L_1 \rightarrow \infty$ . We have checked that these extrapolations are compatible with MF values,  $\nu = 1/2$  and  $\eta = 0$ . We have started with independent fits to the laws  $\nu(L_1) = 1/2 + O(L_1^{-\omega_\nu})$  and  $\eta(L_1) = O(L_1^{-\omega_\eta})$  obtaining

$L_1$	$L_2$	$T_c^\xi$	$T_c^R$
5	6	2.892(6)	2.680(14)
6	7	2.809(16)	2.739(15)
7	8	2.69(4)	2.74(2)

TABLE I. Temperatures for the crossing points of  $\xi/L$  and  $R_{12}$  for consecutive sizes.

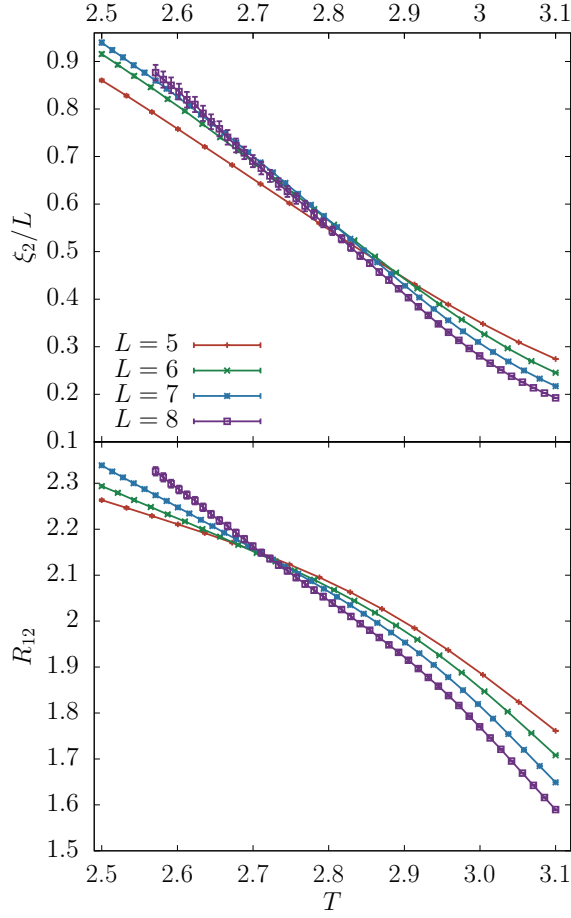


FIG. 2. Second-moment correlation length  $\xi_2$ , Eq. (11), measured in units of the lattice size  $L$  (on the **top**), and dimensionless ratio  $R_{12}$ , Eq. (13) (on the **bottom**), as a function of temperature  $T$ . Both quantities are shown as computed for the replicon propagator, Eq. (2), for all our lattice sizes at  $h = 0.075$ . At the critical point, the curves for different sizes of the system intersect at the same  $T$ , meaning that both  $\xi/L$  and  $R_{12}$  are a scale invariant at  $T_c$ . The presence of a crossing point for  $\xi_2/L$  indicates that the anomalous behaviour of the wave vector  $\mathbf{k} = \mathbf{0}$  is less severe in space dimension  $D = 6$  than previously found at  $D = 4$  [25]. The difference between the crossing points found for both quantities should vanish as  $L \rightarrow \infty$ , since it is due to scaling corrections.

good fits [41]. For  $\nu$  we get  $\chi^2/\text{dof} = 2.9/1$  (dof is the number of degrees of freedom) with a  $p$ -value=9% and  $\omega_\nu = 3.7(1.3)$ . For  $\eta$  we obtain  $\chi^2/\text{dof} = 0.03/1$  with a  $p$ -value=87% and  $\omega_\eta = 1.93(15)$ . We can improve by trying a joint fit for  $\nu$  and  $\eta$  that assumes a common value of  $\omega_{\nu\eta}$  (in agreement with the RG expectation). The joint fit obtains  $\omega_{\nu\eta} = 1.96(15)$  with  $\chi^2/\text{dof} = 5.67/3$  with a  $p$ -value=13%. Our extrapolations to large  $L_1$  not constrained to yield MF exponents resulted in exceedingly large errors for both  $\nu$  and  $\eta$ . Thus, although our data are compatible with an upper critical-dimension in a field  $D_u^h = 6$ , we cannot exclude nearby values for  $D_u^h$ .

At this point, we are ready for a joint extrapolation to

infinite system sizes of the critical temperature reported in Table I using the quotient equation,  $1/T_c - 1/T_c(L) = O(L_1^{-\omega-1/\nu})$ . We obtain in this way:  $T_c = 2.755(13)$  with  $\chi^2/\text{dof} = 5.02/2$  with a  $p$ -value=8.0%.

Finally, let us consider the  $\lambda$  parameter from Eq. (9), that we have computed using the three-, four- and six-replicas estimators of  $\omega_1$  and  $\omega_2$ . These multiple calculations enable us to check two predictions from the RS theory. First, this theory predicts a value of  $\lambda \in [0, 1]$ . Second, it predicts that the three and four replicas estimators gives the true value of  $\lambda$  (which is the one of the six-replicas estimator) near the critical point. Both questions can be addressed from Fig. 3 (we employ dark colors for the values of  $\lambda$  computed with three replicas and light colors for the four-replicas estimator). Notice that the scaling corrections of the three- and four-replicas estimators have opposite signs. Hence we can safely assume that  $\lambda(T_c^+)$  lies between the three- and four-replica estimate of  $\lambda$  for our largest lattice at our estimate of the critical point. In this way, we conclude that  $\lambda(T_c^+) = 0.52(6)$ .

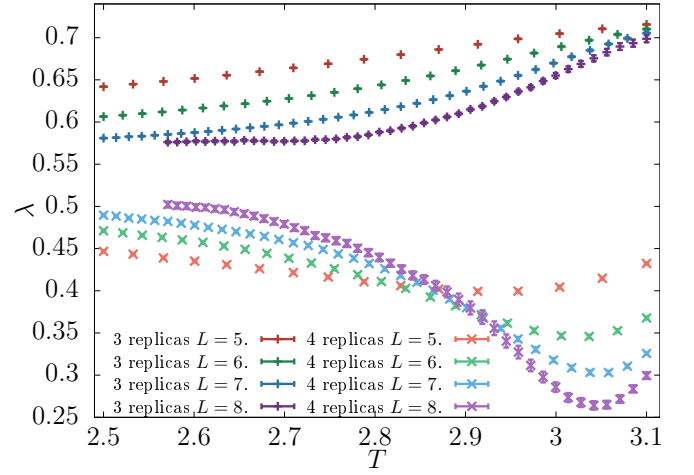


FIG. 3. Three and four-replicas estimators of  $\lambda$ , Eqs. (C6) and (C7), as a function of the temperature. The six-replicas estimator, shown in App. C, turned out to be compatible with—but a lot noisier than—the four-replica estimator. The fact that  $\lambda$  remains bounded illustrates the absence of run-away RG trajectories.

*d. Conclusions.* We have shown strong numerical evidences for a second order phase transition in the six-dimensional Ising spin glass in an external field. Our estimates of critical exponents are compatible with Mean

$L_1$	$L_2$	$\eta(T_c^R)$	$\nu(T_c^R)$
5	6	0.40(1)	0.88(7)
6	7	0.28(1)	0.76(5)
7	8	0.21(1)	0.54(6)

TABLE II. Effective exponents  $\eta$  and  $\nu$  as obtained from the quotient method for lattices  $(L_1, L_2)$ . The table shows the values at the temperatures obtained from the crossings in  $R_{12}$ .

Field, which suggests that the upper critical dimension is  $D_u = 6$ . As explained above, both conclusions contradict many (but not all) previous expectations. However, we do not regard our computation of  $D_u$  as final, because we lack the accuracy for controlling the multiplicative, logarithmic corrections to scaling at  $D_u$  [42, 43] (see App.H for the analysis of the  $h = 0$  phase transition taking into account these log-corrections). Furthermore, by studying the renormalized coupling  $\lambda$ , we have shown that the replicated Replica Symmetric Hamiltonian describes the behavior of the Ising spin glass in a field when the replicon susceptibility takes large values. Our *finite* extrapolation  $\lambda(T_c^+) = 0.52(6) < 1$  is further evidence for a second-order phase transition.

### ACKNOWLEDGMENTS

Our simulations have been carried out in the ADA cluster at the the *Instituto de Computación Científica Avanzada de Extremadura* (ICCAEx), at Badajoz and at the Cierzo cluster at the *Instituto de Biocomputación y Física de Sistemas Complejos* (BIFI) in Zaragoza. We would like to thank both institutions and their staff. This work was partially supported by Ministerio de Ciencia, Innovación y Universidades (Spain), Agencia Estatal de Investigación (AEI, Spain, 10.13039/501100011033), and European Regional Development Fund (ERDF, A way of making Europe) through Grants PID2020-112936GB-I00 and PID2022-136374NB-C21, by the Junta de Extremadura (Spain) and Fondo Europeo de Desarrollo Regional (FEDER, EU) through Grant No. IB20079, by Community of Madrid and Rey Juan Carlos University through Young Researchers program in R&D (Grant CCASSE M2737). J.M.-G. was supported by the Ministerio de Universidades and the European Union ‘NextGenerationEU/PRTR’ through a 2021–2023 Margarita Salas grant.

### Appendix A: The Hamiltonian and the structure of the propagators

The effective Hamiltonian describing the critical behavior of the  $D$ -dimensional Ising spin glass model in presence of a magnetic field  $h$  can be written using the replica framework as [11]

$$\begin{aligned} \mathcal{H} = & \frac{1}{2} \int d^D x \left[ \frac{1}{2} \sum_{ab} (\nabla \phi_{ab})^2 + m_1 \sum_{ab} \phi_{ab}^2 \right. \\ & + m_2 \sum_{abc} \phi_{ab} \phi_{ac} + m_3 \sum_{abcd} \phi_{ab} \phi_{cd} + \\ & \left. - \frac{1}{6} \tilde{w}_1 \sum_{abc} \phi_{ab} \phi_{bc} \phi_{ca} - \frac{1}{6} \tilde{w}_2 \sum_{ab} \phi_{ab}^3 \right]. \quad (\text{A1}) \end{aligned}$$

where, the replicated overlap,  $\phi_{ab}$  is a  $n \times n$  symmetric matrix with zero in the diagonal and  $n$  is the number of

replicas ( $n \rightarrow 0$ ).

The three fundamental modes of the correlation function are named replicon, anomalous and longitudinal modes. The anomalous and longitudinal modes become identical when one takes the limit of vanishing  $n$ . The fundamental propagators of the theory  $G_R(\mathbf{x} - \mathbf{y})$  and  $G_A(\mathbf{x} - \mathbf{y})$  are related to the natural propagators  $G_1(\mathbf{x} - \mathbf{y})$ ,  $G_2(\mathbf{x} - \mathbf{y})$ , and  $G_3(\mathbf{x} - \mathbf{y})$  as

$$\begin{aligned} G_R(\mathbf{x} - \mathbf{y}) &= G_1(\mathbf{x} - \mathbf{y}) - 2G_2(\mathbf{x} - \mathbf{y}) + G_3(\mathbf{x} - \mathbf{y}), \\ G_A(\mathbf{x} - \mathbf{y}) &= G_L(\mathbf{x} - \mathbf{y}) = G_1(\mathbf{x} - \mathbf{y}) - 4G_2(\mathbf{x} - \mathbf{y}) \\ &\quad + 3G_3(\mathbf{x} - \mathbf{y}), \quad (\text{A2}) \end{aligned}$$

where

$$G_1(\mathbf{x} - \mathbf{y}) = \overline{\langle s_{\mathbf{x}} s_{\mathbf{y}} \rangle^2} - q^2, \quad (\text{A3})$$

$$G_2(\mathbf{x} - \mathbf{y}) = \overline{\langle s_{\mathbf{x}} s_{\mathbf{y}} \rangle \langle s_{\mathbf{x}} \rangle \langle s_{\mathbf{y}} \rangle} - q^2, \quad (\text{A4})$$

$$G_3(\mathbf{x} - \mathbf{y}) = \overline{\langle s_{\mathbf{x}} \rangle^2 \langle s_{\mathbf{y}} \rangle^2} - q^2. \quad (\text{A5})$$

with, as usual,  $q = \overline{\langle s_{\mathbf{x}} \rangle^2}$  being the average overlap. Then the correlation functions are defined by

$$G_{\alpha}(\mathbf{x}) = \frac{1}{V} \sum_{\mathbf{y}} G_{\alpha}(\mathbf{x} - \mathbf{y}), \quad \alpha \in \{1, 2, 3, R, L, A\}, \quad (\text{A6})$$

and their Fourier transform

$$\hat{G}_{\alpha}(\mathbf{k}) = \frac{1}{V} \sum_{\mathbf{x}} e^{i\mathbf{k} \cdot \mathbf{x}} G_{\alpha}(\mathbf{x}). \quad (\text{A7})$$

Associated with each two-points correlation functions one can define a susceptibility  $\chi_{\alpha}$  as

$$\chi_{\alpha} = \hat{G}_{\alpha}(\mathbf{0}) \quad \alpha \in \{1, 2, 3, R, L, A\}. \quad (\text{A8})$$

In the particular case of  $h = 0$  case one finds  $\chi_R = \chi_A = \chi_L$  (because  $\chi_2 = \chi_3 = 0$ ). However, as soon as  $h \neq 0$ , the replicon  $\chi_R$  becomes significantly larger than  $\chi_A = \chi_L$  in the spin glass phase. Details on how to compute the correlation functions with a multispin coding algorithm can be found in section F 2 of this Supplemental Material.

### Appendix B: The Helmholtz and Gibbs free energies.

With this Hamiltonian we can compute the associated free energy, the Helmholtz one, defined as

$$F(\lambda_{ab}) = \frac{1}{V} \log \langle e^{\sum_{(ab)} \lambda_{ab} \delta Q_{ab}} \rangle, \quad (\text{B1})$$

where  $(ab)$  denotes sum over  $a \neq b$  and

$$\delta Q_{ab} \equiv Q_{ab} - q, \quad (\text{B2})$$

with

$$Q_{ab} \equiv \frac{1}{V} \sum_{\mathbf{x}} s_{\mathbf{x}}^a s_{\mathbf{x}}^b. \quad (\text{B3})$$

This free energy allows us to compute the average value of the overlap

$$\langle \delta Q_{ab} \rangle = -\frac{\partial F}{\partial \lambda_{ab}}. \quad (\text{B4})$$

The Gibbs free energy,  $G(\delta Q_{ab})$ , is just the Legendre transform of  $F(\lambda_{ab})$  given by

$$G(\delta Q_{ab}) = F(\lambda_{ab}) + \sum_{ab} \lambda_{ab} \delta Q_{ab}, \quad (\text{B5})$$

$\lambda_{ab}$  being a function of  $\delta Q_{ab}$

$$\lambda_{ab} = \frac{\partial G}{\partial \delta Q_{ab}}. \quad (\text{B6})$$

The Taylor expansion of the Helmholtz free energy (up to third order) is

$$\begin{aligned} F(\lambda) = & -\frac{1}{2} \sum_{(ab)} G_{ab,cd} \lambda_{ab} \lambda_{cd} \\ & -\frac{1}{6} \sum_{(ab),(cd),(ef)} \mathcal{W}_{ab,cd,ef} \lambda_{ab} \lambda_{cd} \lambda_{ef}. \end{aligned} \quad (\text{B7})$$

The coefficients  $\mathcal{W}_{ab,cd,ef}$  can take only eight different values in a RS phase, namely:  $\mathcal{W}_{ab,bc,ca} = \mathcal{W}_1$ ,  $\mathcal{W}_{ab,ab,ab} = \mathcal{W}_2$ ,  $\mathcal{W}_{ab,ab,ac} = \mathcal{W}_3$ ,  $\mathcal{W}_{ab,ab,cd} = \mathcal{W}_4$ ,  $\mathcal{W}_{ab,ac,bd} = \mathcal{W}_5$ ,  $\mathcal{W}_{ab,ac,ad} = \mathcal{W}_6$ ,  $\mathcal{W}_{ac,bc,de} = \mathcal{W}_7$ , and  $\mathcal{W}_{ab,cd,ef} = \mathcal{W}_8$ .

In terms of these  $\mathcal{W}_i$  ( $i = 1, \dots, 8$ ) the cubic part of the Helmholtz free energy can be written as

$$\begin{aligned} & \sum_{(ab),(cd),(ef)} \mathcal{W}_{ab,cd,ef} \lambda_{ab} \lambda_{cd} \lambda_{ef} \\ = & \omega_1 \sum_{abc} \lambda_{ab} \lambda_{bc} \lambda_{ca} + \omega_2 \sum_{ab} \lambda_{ab}^3 + \omega_3 \sum_{abc} \lambda_{ab}^2 \lambda_{ac} \\ & + \omega_4 \sum_{abcd} \lambda_{ab}^2 \lambda_{cd} + \omega_5 \sum_{abcd} \lambda_{ab} \lambda_{ac} \lambda_{bd} + \omega_6 \sum_{abcd} \lambda_{ab} \lambda_{ac} \lambda_{ad} \\ & + \omega_7 \sum_{abcde} \lambda_{ac} \lambda_{bc} \lambda_{de} + \omega_8 \sum_{abcdef} \lambda_{ab} \lambda_{cd} \lambda_{ef}. \end{aligned} \quad (\text{B8})$$

We quote here only the relationship between  $\omega_1$  and  $\omega_2$  (the two relevant terms in this context [29]) and the  $\mathcal{W}_i$ :

$$\begin{aligned} \omega_1 &= \mathcal{W}_1 - 3\mathcal{W}_5 + 3\mathcal{W}_7 - \mathcal{W}_8, \\ \omega_2 &= \frac{1}{2}\mathcal{W}_2 - 3\mathcal{W}_3 + \frac{3}{2}\mathcal{W}_4 + 3\mathcal{W}_5 + 2\mathcal{W}_6 - 6\mathcal{W}_7 + 2\mathcal{W}_8. \end{aligned} \quad (\text{B9})$$

that can be expressed as:

$$\begin{aligned} \omega_1 &= \frac{1}{V} \sum_{xyz} \overline{\langle s_x s_y \rangle_c \langle s_y s_z \rangle_c \langle s_z s_x \rangle_c}, \\ \omega_2 &= \frac{1}{2V} \sum_{xyz} \overline{\langle s_x s_y s_z \rangle_c^2}, \end{aligned} \quad (\text{B10})$$

where by  $\langle \langle \dots \rangle \rangle_c$  we denote connected correlation functions. Notice that the coefficients of the terms of order  $O(\lambda^m)$  in the expansion of the Helmholtz free energy,  $F(\lambda)$ , are the  $m$ -term connected susceptibilities.

At this point the Gibbs free energy can be written as

$$\begin{aligned} G(\delta Q) &= \frac{1}{2} \sum_{(ab),(cd)} \delta Q_{ab} M_{ab,cd} \delta Q_{cd} \\ &\quad - \frac{w_1}{6} \sum_{abc} \delta Q_{ab} \delta Q_{bc} \delta Q_{ca} - \frac{w_2}{6} \sum_{ab} \delta Q_{ab}^3. \end{aligned} \quad (\text{B11})$$

Observe that the cubic coupling in the Hamiltonian are written as  $\tilde{w}_1, \tilde{w}_2$  and they are different from the coefficients  $w_1, w_2$  of the Gibbs Free energy [29] (the so-called vertices in field theoretical language). The coefficients  $\tilde{w}_i$  and  $w_i$  are, respectively, the bare and dressed couplings. The bare and dressed couplings generally differ, they are only equal at the level of the tree approximation in field theory.

### Appendix C: The parameter $\lambda$

A good way to characterize the nature of the transition is by means of the parameter  $\lambda$  defined as

$$\lambda = \frac{w_2}{w_1}, \quad (\text{C1})$$

where  $w_1$  and  $w_2$  are the coefficients (i.e exact vertices) of the static replicated Gibbs free energy [29]. It can be shown that the exact vertices can be expressed as [29]

$$w_i = \frac{\omega_i}{\chi_R^3} \quad (i = 1, 2). \quad (\text{C2})$$

Hence, it follows that  $\lambda = \omega_2/\omega_1$ .

In addition the  $\lambda$  parameter does not renormalize. The three-point renormalized constants  $w_{1,r}$  and  $w_{2,r}$  are defined in the usual way

$$w_{i,r} = \frac{\omega_i}{\chi_R^{3/2} \xi_2^{D/2}}, \quad (i = 1, 2), \quad (\text{C3})$$

therefore

$$\lambda_r = \frac{w_{2,r}}{w_{1,r}} = \frac{\omega_2}{\omega_1} = \frac{w_2}{w_1} = \lambda. \quad (\text{C4})$$

The parameter  $\lambda$  is also related with the cubic couplings  $\tilde{w}_1$  and  $\tilde{w}_2$  of the Replica Symmetric Hamiltonian of Bray and Roberts [10] since, at mean field (MF) level, we have  $\tilde{w}_i = w_i$  ( $i = 1, 2$ ). Then,  $\lambda$  signals the breaking point from RS to Replica Symmetry Breaking. For further details see Refs. [24, 29].

In numerical simulations we compute the parameters

$\omega_1$  and  $\omega_2$  using Eq. (B9) with the  $\mathcal{W}_i$  given by [29]

$$\begin{aligned}\mathcal{W}_1 &\equiv V^2 \langle \delta Q_{12} \delta Q_{23} \delta Q_{31} \rangle, \\ \mathcal{W}_2 &\equiv V^2 \langle \delta Q_{12}^3 \rangle, \\ \mathcal{W}_3 &\equiv V^2 \langle \delta Q_{12}^2 \delta Q_{13} \rangle, \\ \mathcal{W}_4 &\equiv V^2 \langle \delta Q_{12}^2 \delta Q_{34} \rangle, \\ \mathcal{W}_5 &\equiv V^2 \langle \delta Q_{12} \delta Q_{13} \delta Q_{24} \rangle, \\ \mathcal{W}_6 &\equiv V^2 \langle \delta Q_{12} \delta Q_{13} \delta Q_{14} \rangle, \\ \mathcal{W}_7 &\equiv V^2 \langle \delta Q_{12} \delta Q_{13} \delta Q_{45} \rangle, \\ \mathcal{W}_8 &\equiv V^2 \langle \delta Q_{12} \delta Q_{34} \delta Q_{56} \rangle,\end{aligned}\tag{C5}$$

and the overlap fluctuations  $\delta Q_{ab}$  can be computed in terms of independent real replicas ( $a$  and  $b$ ) using Eq. (B2).

To compute each cubic cumulant  $\mathcal{W}_i$  requires a number of different real replicas equal to the largest index in its expression. The RS field theory predicts that the amplitudes of the  $\{\mathcal{W}_1, \dots, \mathcal{W}_8\}$  set are not independent [29]. Using the linear relationship between them one can compute  $\omega_1$  and  $\omega_2$  in terms of three- and four-replicas estimators. In particular, the three-replicas estimators are [29]

$$\begin{aligned}\omega_1^{(3)} &\equiv \frac{11}{30} \mathcal{W}_1 + \frac{2}{15} \mathcal{W}_2, \\ \omega_2^{(3)} &\equiv \frac{4}{15} \mathcal{W}_1 - \frac{1}{15} \mathcal{W}_2,\end{aligned}\tag{C6}$$

and the four-replicas ones [29]

$$\begin{aligned}\omega_1^{(4)} &\equiv \frac{23\mathcal{W}_1}{30} + \frac{\mathcal{W}_2}{20} - \frac{3\mathcal{W}_3}{5} + \frac{9\mathcal{W}_4}{20} - \frac{6\mathcal{W}_5}{5} + \frac{\mathcal{W}_6}{2}, \\ \omega_2^{(4)} &\equiv \frac{7\mathcal{W}_1}{15} + \frac{2\mathcal{W}_2}{5} - \frac{9\mathcal{W}_3}{5} + \frac{3\mathcal{W}_4}{5} - \frac{3\mathcal{W}_5}{5} + \mathcal{W}_6.\end{aligned}\tag{C7}$$

Within the framework of the RS theory, the values of the three- and four-replicas estimators differ in general from the true values of  $\omega_1$  and  $\omega_2$  but coincide with them at the critical temperature [29]. This gives us the opportunity to check the validity of the RS theory by computing the three-, four- and six-replicas estimators.

### 1. $\lambda$ infinite-temperature limit

As a part of our analysis of the behaviour of the observable  $\lambda$ , we have studied how far from the infinite-temperature limit our results are. In this section we show the computations of  $\lambda$  in the infinite-temperature limit for three, four and six replicas.

Actually, the computation of  $\lambda$  at infinite temperature is reduced to the computation of the cubic cumulants  $\mathcal{W}_i$  with  $i \in \{1, 2, \dots, 8\}$  in the same regime.

Let us start by computing the very simple case of the cumulant  $\mathcal{W}_2$ . Starting from the expression of the cumulant given by Eq. (C5) and Eq. (B2) we can develop the

expression of  $\mathcal{W}_2$ :

$$\begin{aligned}\mathcal{W}_2 &= V^2 \langle (Q_{12} - q)^3 \rangle = \\ &= V^2 \langle Q_{12}^3 \rangle - 3q \langle Q_{12}^2 \rangle + 2V^2 q^3.\end{aligned}\tag{C8}$$

In the infinite-temperature limit in which we are interested of, the value of  $q$  tends to 0, so the only relevant term is  $V^2 \langle Q_{12}^3 \rangle$ . Expanding this term we get

$$\langle Q_{12}^3 \rangle = \frac{1}{V^3} \sum_{\mathbf{x}\mathbf{y}\mathbf{z}} \langle s_{\mathbf{x}}^1 s_{\mathbf{x}}^2 s_{\mathbf{y}}^1 s_{\mathbf{y}}^2 s_{\mathbf{z}}^1 s_{\mathbf{z}}^2 \rangle.\tag{C9}$$

In the infinite-temperature limit, the only relevant terms are those with  $\mathbf{x} = \mathbf{y} = \mathbf{z}$ . Other possibilities vanish when thermal averages are taken since thermal fluctuations are dominant in that regime. Thus, we have

$$\langle Q_{12}^3 \rangle_{T \rightarrow \infty} = \frac{1}{V^3} \sum_{\mathbf{x}} \langle s_{\mathbf{x}}^1 s_{\mathbf{x}}^2 s_{\mathbf{x}}^1 s_{\mathbf{x}}^2 s_{\mathbf{x}}^1 s_{\mathbf{x}}^2 \rangle.\tag{C10}$$

Spins appearing an odd number of times lead to cancellations in the Eq. (C10) when thermal averages are taken. On the contrary, spins appearing an even number of times can pair each other and contribute one unit to the sum.

This simple reasoning indicate us that, each time a replica is appearing an odd number of times in the expression of  $\mathcal{W}_i$ , that cubic cumulant will be 0 in the infinite-temperature limit. That is the case for  $\mathcal{W}_i$  with  $i \geq 2$ . However, for  $\mathcal{W}_1$  we have

$$\mathcal{W}_1 = V^2 \langle Q_{12} Q_{23} Q_{31} \rangle - 3q \langle Q_{12} Q_{13} \rangle + 2V^2 q^3.\tag{C11}$$

In Eq. (C11), the only non-zero term in the infinite limit, the first one, contains an even number of spins of each replica when expanding it. Therefore, this term will contribute with a factor 1 when averages are taken. Then,  $\mathcal{W}_1 = 1$  and  $\mathcal{W}_i = 0$  for  $i \geq 2$  in the infinite-temperature limit.

At this point, the computation of  $\lambda$  is easy. From Eq. (C1) we obtain

$$\lambda = \frac{\omega_2}{\omega_1} = 0.\tag{C12}$$

Similar computations are valid for the three-replicas and four-replicas cases. From Eqs. (C6) and Eqs. (C7) we have

$$\lambda^{(3)} = \frac{\omega_2^{(3)}}{\omega_1^{(3)}} = \frac{8}{11},\tag{C13}$$

$$\lambda^{(4)} = \frac{\omega_2^{(4)}}{\omega_1^{(4)}} = \frac{14}{23}.\tag{C14}$$

## 2. Comparison of $\lambda$ computed with three, four and six replicas

We represent in Fig. 4 the three-, four- and six-replicas estimator of  $\lambda$ . We also plot the infinite temperature values for three and four replicas. The three-replicas estimator seems to converge to the infinite value faster than the four-replicas estimator, which exhibit a crossover between the six-replicas behavior at low temperatures and the infinite temperature one at higher temperatures.

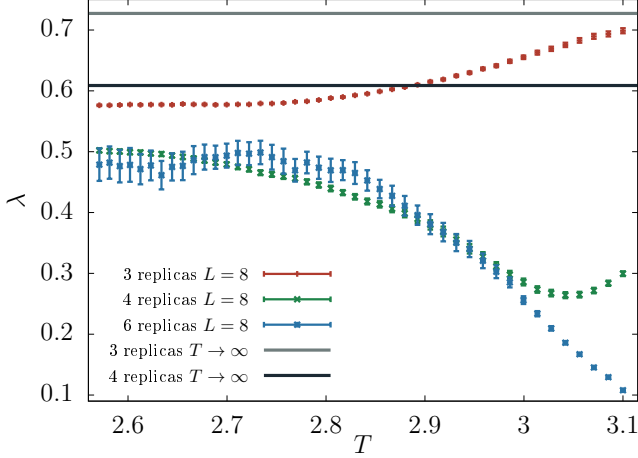


FIG. 4. Plot of the three-, four- and six-replicas estimator of  $\lambda$ , Eqs. (C6), (C7) and (B9) respectively, as a function of the temperature. We also plot the infinite temperature limits for three and four replicas.

In Fig. 5 we show the values of six-replicas estimator of  $\lambda$  as a function of the temperature for different lattice sizes.

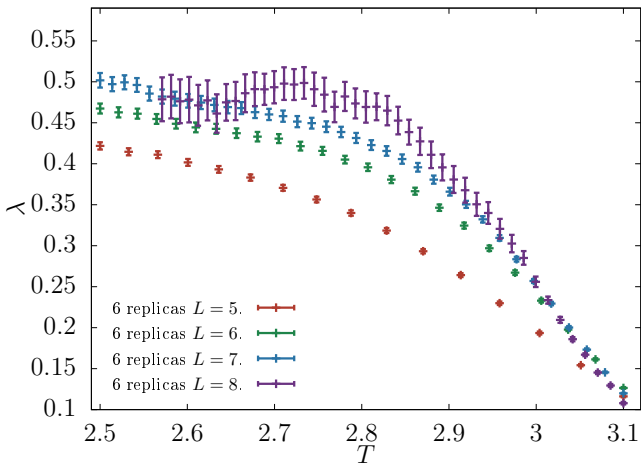


FIG. 5. Plot of the six-replicas estimator of  $\lambda$ , Eq. (B9) and (C4), as a function of the temperature for all the lattice sizes  $L$ .

## 3. $\Lambda$ cumulants

One could have addressed the computation of the two renormalized constants  $w_{i,r}$  ( $i = 1, 2$ ), however, they presents strong finite-size effects. Instead, we have resorted to the computation of the  $\Lambda_i$  cumulants introduced in Ref. [24]

$$\Lambda_i = \frac{\omega_i}{\chi_R^{3/2} L^{D/2}} \text{ with } i \in \{1, 2\}. \quad (\text{C15})$$

The  $\Lambda_i$  cumulants scales in the same way as a dimensionless observable, like the Binder cumulant or  $\xi_2/L$ .

In Figs. 6 and 7 one can find a two panel figure for  $\omega_1$ ,  $\Lambda_1$ , and for  $\omega_2$ ,  $\Lambda_2$  respectively as a function of  $T/T_c$ .

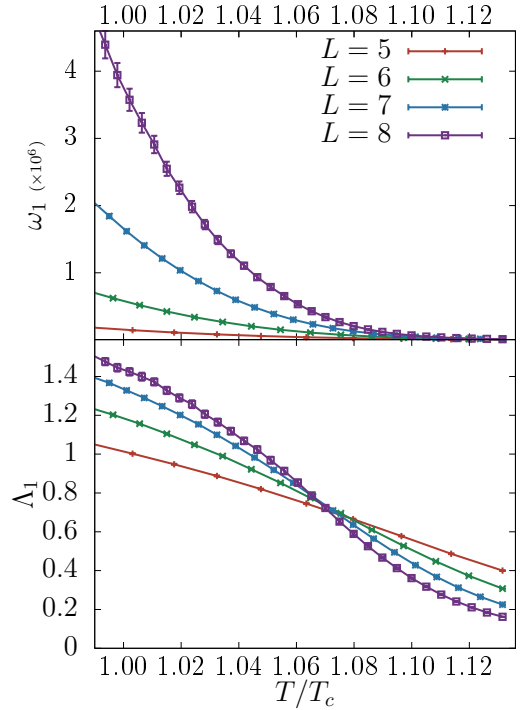


FIG. 6. Plot of  $\omega_1$  (on the **top**), Eq. (B9), and the cumulant  $\Lambda_1$  (on the **bottom**), Eq. (C15), as a function of  $T/T_c$ .

Notice that both  $\Lambda$ -cumulants show crossing points (better signal for  $\Lambda_1$ ), as expected, drifting very slowly to the critical point.

In addition the connected susceptibilities  $\omega_1$  and  $\omega_2$  diverge in the critical region as predicted by the theory:  $\omega_{1,2} \propto |T - T_c|^{-\gamma_3}$  with  $\gamma_3 = 6\nu - \frac{3}{2}\nu\eta$  in six dimensions [24] ( $\gamma_3 = 3$  for  $D = 6$  and the MF exponents).

## Appendix D: Probability density function of the overlaps

We have computed the probability density function of the overlap,  $q$ , for  $L = 6$  and  $L = 8$ . We observe (see Fig. 8) for both lattice sizes that the probability density



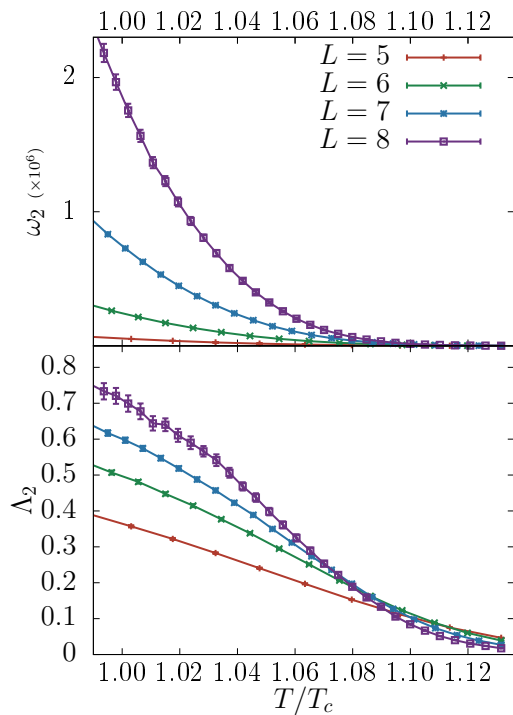


FIG. 7. **Up:** Plot of  $\omega_2$  as a function of  $T/T_c$ . **Down:** Plot of  $\Lambda_2$  as a function of  $T/T_c$ .

function is non-zero for negative overlaps. Note that the tail at  $q < 0$  is suppressed in the thermodynamic limit. Indeed, the trend towards a suppression of the tail as  $L$  grows is very clear from our data in Fig. 8.

As mentioned in the main text, the non-negligible tail of negative overlaps is probably responsible of the undesirable behavior of the propagator at wave vector  $\mathbf{k} = \mathbf{0}$ , which makes it difficult to find intersections of the curves corresponding to different (small) lattice sizes of  $\xi_2/L$  as a function of temperature.

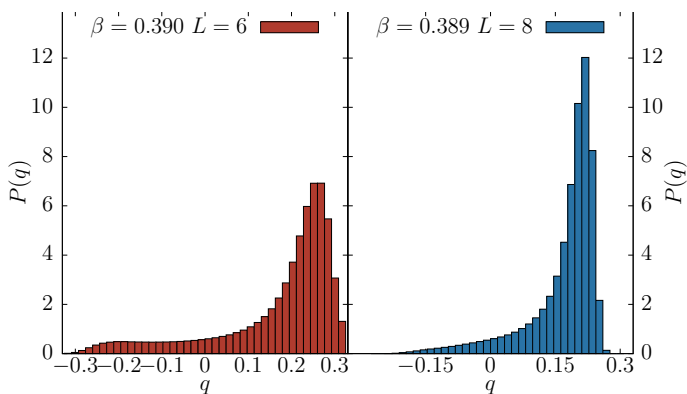


FIG. 8. Probability density function of the overlap  $P(q)$  for two different sizes:  $L = 6$  (left) and  $L = 8$  (right). We have computed  $P(q)$  for the lowest available temperature for  $L = 8$  ( $\beta \approx 0.389$ ) and the closest available temperature for  $L = 6$  ( $\beta \approx 0.390$ ).

## Appendix E: Numerical simulation details

To study the six dimensional Ising spin glass in the presence of a magnetic field we have written several computer programs in C language. In our simulations, we use an offline analysis approach, meaning our simulation program writes configurations of spins and then a different analysis program computes the correlation lengths and other magnitudes of interest. Finally, a third program is in charge of the statistical analysis of the data, using the Jackknife technique [44, 45]. It is worth mentioning that both, the simulation and the analysis program, make use of the POSIX thread libraries, which allow us to create different threads that run parallel on different cores.

We have simulated the Edwards-Anderson model in a six dimensional hypercube with periodic boundary conditions, using a multispin coding Monte Carlo simulation and performing a parallel tempering [32, 33] proposal every 20 Monte Carlo Sweeps (MCS). For each sample, we have simulated 6 replicas. The sizes of the side  $L$  of the hypercube range from  $L = 5$  to  $L = 8$ . The value of the magnetic field  $h$  has been set to  $h = 0.075$ . The number of samples used to obtain the results that we present can be consulted in Table III, along with some other information about the simulations.

$L$	#Samples	#Temp.	$T_{\min}$	$T_{\max}$	ps/spin flip
5	25600	16	2.50	3.10	16
6	25600	24	2.50	3.10	12
7	25600	36	2.50	3.10	20
8	5120	48	2.57	3.10	16

TABLE III. Some parameters of our simulation. The first column refers to the size of the side of the hypercube. In the second column we present the number of samples analyzed. The third column shows the number of temperatures simulated for each size. This number have been chosen in a way that ensures the random walk in temperatures to be sufficiently ergodic. The fourth and fifth columns refers to the lower and upper values of the temperature interval. Finally, the last column shows the number of picoseconds (ps) per spin flip of the simulation.

To ensure that we measure the equilibrium properties of the system, the thermalization of each sample must be studied individually. We have designed a thermalization protocol based on Ref. [34] that works in the following way.

First we simulate our super-sample (a package of 128 samples) during a sufficiently large number of MCS for most of the samples to be thermalized. This value  $N_{\text{sim}}$  was determined by preliminary runs. During the simulation, the random walk in temperatures induced by the parallel tempering algorithm for each of the 128 samples is registered. Then, when the simulation ends, we study this random walk, and compute from it the integrated autocorrelation time  $\tau_{\text{int},f}$  for several magnitudes  $f$ , related with the random walks [34]. We take the largest of these integrated autocorrelation times,  $\tau_{\text{int},f*}$ , and make

the assumption  $\tau_{\text{int},f*} \sim \tau_{\text{exp}}$ . The value of the exponential autocorrelation time enables us to check if a given sample is thermalized. In particular, we consider a sample to be thermalized if its simulation time  $\tau_{\text{sim}}$  is forty times bigger than  $\tau_{\text{exp}}$  (i.e  $N_{\text{sim}} > 30\tau_{\text{exp}}$ ).

When in a super-sample a non-equilibrated sample is found, we proceed as follows. The last configurations of those samples which are not thermalized are extracted from the corresponding super-sample. Then a new super-sample is built grouping non-thermalized samples and their simulation time is doubled. Finally, the thermalization check is repeated,  $\tau_{\text{exp}}$  is measured, and if the criteria is not fulfilled, the simulations are extended once again. This process is repeated until all samples reach their equilibrium states. At the end, the samples are reintroduced into their original super-samples, ready to be analyzed.

## Appendix F: Details of multispin coding algorithms

One of the most complex task we have faced when trying to generate the results that we present here is the elaboration of coding algorithms. In this appendix we show some examples that can give a taste of how the problem is approached.

### 1. Metropolis algorithm

Current CPUs are able to execute one-clock-cycle instructions over registers (or words) of 128 bits. The 128-bits words are coded by using the Intel Intrinsics' [46] variables `_m128i` consisting in 128 Boolean variables. We benefit from this 128-bits words by simulating at once 128 samples.

Let us define a vector  $S[V]$  of type `_m128i`, where  $V$  is the number of spins of our system. Each element of the vector  $S[i]$ , contains 128 Boolean variables representing the value of the spin at the  $i$ -th position for the 128 samples. Analogously, we can define a vector  $J[6*V]$  in which each element  $J[i]$  contains the value of the coupling for the 128 samples at the  $i$ -th position. Now, the problem reduces to code the Metropolis algorithm in bit-wise operations to improve the performance up to 128 times. We work with the following assignment

$$s = +1 \rightarrow b_s = +1, \text{ and } s = -1 \rightarrow b_s = 0, \quad (F1)$$

$$J = +1 \rightarrow b_J = 0 \text{ and } J = -1 \rightarrow b_J = 1, \quad (F2)$$

where the  $b$  variables are the bit variable of our program. This seemingly arbitrary election has a virtue: the equivalence

$$b_{s1} \wedge b_J \wedge b_{s2} = (1 - J s_1 s_2)/2, \quad (F3)$$

where  $\wedge$  represents the Boolean *exclusive or* (XOR).

We use a variation from the original Metropolis algorithm to decide if a given spin is flipped or not. The Hamiltonian is composed by an interaction term  $\mathcal{H}_J$  and a magnetic field term  $\mathcal{H}_h$ . The probability of performing a given spin flip is determined by the product

$$\min\{1, \exp(-\Delta\mathcal{H}_J)\} \min\{1, \exp(-\Delta\mathcal{H}_h)\}. \quad (F4)$$

This election is not completely equivalent to the standard Metropolis algorithm, but it verifies the detailed balance condition and has the virtue of simplifying the implementation. One can execute this spin flip simultaneously for the 128 samples having an `_m128i` variable `flip` which encodes the information. If the spin from the  $i$ -th sample must be flipped, then `flipi` = 1, if it must remain in the same position `flipi` = 0. Then one can carry out the flip decision simultaneously using the XOR operator

$$S[\text{site}] = S[\text{site}] \wedge \text{flip}[\text{site}]. \quad (F5)$$

The `flip` variable has two different contributions, one coming from the difference in the interaction energy considering the spin neighbours, `flipJ`, and other coming from the spin alignment with the field  $h$ , `fliph`, so that

$$\text{flip} = \text{flipJ} \& \text{flip}_h. \quad (F6)$$

Since we only consider nearest-neighbour interactions this energy difference coming from the interactions with neighbours term will be

$$\Delta\mathcal{H}_J = -2s_x \sum_y J_{xy} s_y, \quad (F7)$$

where the sum is restricted over the 12 neighbours of  $s_x$ . In the  $\{+1, -1\}$  base the energy difference  $\Delta\mathcal{H}_J$  can take 12 values ranging from  $-24$  to  $+24$  in steps of 4. To compute  $\Delta E_J$  in the bit base  $\{0, 1\}$  we define  $n_{\text{un}}$ , which represent the number of unsatisfied couplings of a given spin. The maximum possible value of  $n_{\text{un}}$  is 12, and the energy difference is  $\Delta\mathcal{H}_J = 24 - 2n_{\text{un}}$ . To compute  $n_{\text{un}}$  we select a given spin  $S[\text{site}]$  and check if a given coupling is satisfied using Eq. (F3). This information is then encoded in eight 128-bit variables. To account for the heat bath effect, we generate a random number  $R \in [0, 1)$  and check if  $R < \exp(-\beta\Delta\mathcal{H}_J)$  for each sample. We use the same random number for all samples, so we can check if it surpass a barrier of  $\exp(-4\beta)$ ,  $\exp(-8\beta)$ , ...,  $\exp(-24\beta)$ . The number of barriers surpassed are encoded in three new `_m128i` variables named `id1`, `id2`, `id3`. We assign `flipJ` a value of one if

$$\text{id1} + 2\text{id2} + 4\text{id3} + n_{\text{un}} \geq 6 \quad (F8)$$

Computationally, taking this decision takes a total of 54 Boolean operations.

Finally one check if after the flip the spin is aligned with the field  $h$ , and if so make the assignment `fliph` = 1. This process is repeated for every spin of the system.

## 2. Multispin coding for correlation functions

Our goal is to compute the correlation functions  $G_R(x)$  and  $G_A(x)$  as defined in section A. For convenience, we define two new propagators  $\Gamma_1$  and  $\Gamma_2$  as

$$\Gamma_1(\mathbf{x} - \mathbf{y}) = \overline{\langle (s_{\mathbf{x}} - \langle s_{\mathbf{x}} \rangle) (s_{\mathbf{y}} - \langle s_{\mathbf{y}} \rangle) \rangle}, \quad (\text{F9})$$

$$\Gamma_2(\mathbf{x} - \mathbf{y}) = \overline{\langle s_{\mathbf{x}} s_{\mathbf{y}} \rangle} - \overline{\langle s_{\mathbf{x}} \rangle^2 \langle s_{\mathbf{y}} \rangle^2}. \quad (\text{F10})$$

It can be easily shown that

$$G_R(\mathbf{x} - \mathbf{y}) = \Gamma_1(\mathbf{x} - \mathbf{y}), \quad (\text{F11})$$

and

$$G_A(\mathbf{x} - \mathbf{y}) = 2\Gamma_1(\mathbf{x} - \mathbf{y}) - \Gamma_2(\mathbf{x} - \mathbf{y}), \quad (\text{F12})$$

so it is enough for us to compute  $\Gamma_1$  and  $\Gamma_2$  in order to obtain the replicon and anomalous propagators. They can be computed with the help of replicas as

$$\Gamma_1(\mathbf{x} - \mathbf{y}) = \overline{\langle \varphi_{ab;cd}(\mathbf{x}) \varphi_{ab;cd}(\mathbf{y}) \rangle}, \quad (\text{F13})$$

$$\Gamma_2(\mathbf{x} - \mathbf{y}) = \overline{\langle \Delta_{ab;cd}(\mathbf{x}) \Delta_{ab;cd}(\mathbf{y}) \rangle}, \quad (\text{F14})$$

where

$$\varphi_{ab;cd}(\mathbf{x}) = \frac{(s_{\mathbf{x}}^a - s_{\mathbf{x}}^b)(s_{\mathbf{x}}^c - s_{\mathbf{x}}^d)}{2}, \quad (\text{F15})$$

$$\Delta_{ab;cd}(\mathbf{x}) = \frac{(q_{\mathbf{x}}^{ab} - q_{\mathbf{x}}^{cd})}{\sqrt{2}}. \quad (\text{F16})$$

Notice that one need at least 4 replicas to compute the two points connected correlation functions estimators. We would like to evaluate the fields  $\varphi_{ab;cd}(x)$  and  $\Delta_{ab;cd}(x)$  simultaneously for the 128 systems, so we are forced to do it just using Boolean operations. One can easily check that  $\varphi_{ab;cd}(x)/2$  can take three values:  $+1, 0, -1$ . Then, its value can be completely determine using three auxiliary Boolean variables defined as

$$\varphi_1 = (s^a \wedge s^b) \& (s^c \wedge s^d), \quad (\text{F17})$$

$$\varphi_2 = (s^a \wedge s^d), \quad (\text{F18})$$

$$\varphi_3 = \varphi_1 \& \varphi_2. \quad (\text{F19})$$

In particular,  $\varphi_1 = 1$  if the field in this point  $\varphi_{ab;cd}(x)/2$  is not zero and  $\varphi_3 = 1$  if it is  $+1$ . Then one can compute the value of the field in a given hyper-plane  $P$  using a Boolean sum function and computing

$$\frac{1}{2} \sum_{x \in P} \varphi_{ab;cd}(x) = 2 \sum_{x \in P} \varphi_3(x) - \sum_{x \in P} \varphi_1(x). \quad (\text{F20})$$

To compute  $\Delta_{ab;cd}(x)$  one proceeds in a similar way. In particular, the auxiliary Boolean variables are

$$\Delta_1 = (s^a \wedge s^b) \wedge (s^c \wedge s^d), \quad (\text{F21})$$

$$\Delta_2 = \Delta_1 \& (s^c \wedge s^d). \quad (\text{F22})$$

The value of  $\Delta_1(x)$  tells you if  $\Delta_{ab;cd}(x)/\sqrt{2}$  is  $+1$  and  $\Delta_2$  if it is not zero.

## Appendix G: Computing the critical exponents

The value of the critical exponents can be estimated using the quotient method. Usually, the exponent  $\eta$  would be extracted from the replicon susceptibility  $\chi_R$ , but to avoid the problematic  $\mathbf{k} = \mathbf{0}$  wave vector we compute it from  $\mathcal{F}$  as defined in the Eq. (14) of the main article, which has the same scaling behaviour of  $\chi_R$ . The quotient method idea is to compute

$$\mathcal{Q}_{\mathcal{F}} = \frac{\mathcal{F}^{L_2}(T_c)}{\mathcal{F}^{L_1}(T_c)} = \left( \frac{L_2}{L_1} \right)^{2-\eta} + \dots, \quad (\text{G1})$$

and then, to leading order,

$$\eta = 2 - \frac{\log \mathcal{Q}_{\mathcal{F}}}{\log(L_2/L_1)}. \quad (\text{G2})$$

From our data we can obtain an estimation of  $\eta$ , given the three combinations of increasing values  $L_1$  and  $L_2$ .

The  $\nu$  exponent can also be computed by using the quotient method. A standard way to do it would be studying the correlation length derivative with respect to the inverse temperature  $\beta$ . However, once again we avoid the  $\mathbf{k} = \mathbf{0}$  mode and compute  $\nu$  by means of the derivative of the  $R_{12}$ , defined in Eq. (13) of the main article, as

$$\mathcal{Q}_{\partial_{\beta} R} = \frac{\partial_{\beta} R_{12}^{L_2}(T_c)}{\partial_{\beta} R_{12}^{L_1}(T_c)} = \left( \frac{L_2}{L_1} \right)^{1/\nu} + \dots, \quad (\text{G3})$$

$$\nu = \frac{\log(L_2/L_1)}{\mathcal{Q}_{\partial_{\beta} R}}. \quad (\text{G4})$$

The values of  $\partial_{\beta} R_{12}$  have been obtained by deriving a polynomial fit of the sixth degree of  $R_{12}$ .

Finally, the critical temperature have also been computed by using the quotient method. We estimate the critical temperature as the crossing temperature between curves of  $\xi/L$  for consecutive  $L$  and also as the crossing temperature between curves of  $R_{12}$ , also for consecutive  $L$ . With those data, appearing in Tab. I of the main text, we perform a join fit with the two data set to

$$\beta_c^L = \beta_c^{\infty} + A \frac{s^{-\omega} - 1}{1 - s^{1/\nu}} L^{-\omega-1/\nu}, \quad (\text{G5})$$

where  $\beta = 1/T$ ,  $s = (L+1)/L$  and  $\nu$  is fixed to  $\nu = 1/2$ .

The results of the fit are given in the main text and we repeat them here for convenience:  $T_c = 1/\beta_c^{\infty} = 2.755(13)$  with  $\chi^2/\text{dof} = 5.02/2$  with a  $p$ -value=8.0%.

We have also checked that the impact of the factor  $f(s) = (s^{-\omega} - 1)/(1 - s^{1/\nu})$  is negligible. Actually, if we perform the same fit setting  $f(s) = 1$  we obtain:  $T_c = 1/\beta_c^{\infty} = 2.755(15)$  with  $\chi^2/\text{dof} = 5.48/2$  with a  $p$ -value=6.5%.

## Appendix H: The $h = 0$ transition

### 1. Theory

As a previous step to the analysis of our system, we have studied the six-dimensional model of an Ising spin glass without a magnetic field, described by the Hamiltonian

$$\mathcal{H} = - \sum_{\langle \mathbf{x}, \mathbf{y} \rangle} J_{\mathbf{x}\mathbf{y}} s_{\mathbf{x}} s_{\mathbf{y}}, \quad (\text{H1})$$

where  $J_{\mathbf{x}\mathbf{y}} = \pm 1$  with equal probabilities,  $s_{\mathbf{x}}$  are Ising spin variables and the sum is restricted over nearest neighbours. The system has been studied by means of standard numerical Metropolis Monte Carlo simulations (with a non-multispin coding program) and the help of the parallel tempering algorithm. We check the existence of a phase transition by computing the Binder cumulant, defined as

$$g = 1 - \frac{\overline{\langle q_J^4 \rangle}}{3 \overline{\langle q_J^2 \rangle}^2}, \quad (\text{H2})$$

where the overlap computed in a given sample,  $q_J$ , is

$$q_J = \frac{1}{V} \sum_{\mathbf{x}} s_{\mathbf{x}} \tau_{\mathbf{x}}, \quad (\text{H3})$$

where  $\{s_{\mathbf{x}}\}$  and  $\{\tau_{\mathbf{x}}\}$  are, as usual, two replicas of the system evolving with the same disorder but different initial conditions. The correlation length  $\xi_2$  is defined using the two point (non-connected) correlation function

$$G(\mathbf{x} - \mathbf{y}) = \overline{\langle s_{\mathbf{x}} s_{\mathbf{y}} \rangle^2}. \quad (\text{H4})$$

We check the values of the critical exponents and, since we are at the upper critical dimension  $D_U$ , we also check the values of the logarithmic corrections.

In the presence of logarithmic corrections, the scaling laws near the critical point for the correlation length and the susceptibility must be modified as [7, 47]

$$\xi_2 \sim |t|^{-\nu} |\log |t||^{\hat{\nu}}, \quad (\text{H5})$$

$$\chi_{SG} \sim |t|^{-\gamma} |\log |t||^{\hat{\gamma}}. \quad (\text{H6})$$

At the infinite volume critical point, the correlation length defined on a box of size  $L$  behaves as [47]

$$\xi_2 \sim L(\log L)^{\hat{q}}, \quad (\text{H7})$$

and the susceptibility

$$\chi_{SG} \sim L^{2-\eta} (\log L)^{\hat{a}}, \quad (\text{H8})$$

so the complete scaling behaviour for the six dimensional spin glass of  $\xi/L$  and  $\chi$  is [43]

$$\xi_2/L = |\log L|^{\hat{q}} f_{\xi} \left( L^2 t / (\log L)^{4/3} \right), \quad (\text{H9})$$

and

$$\chi_{SG} = L^2 |\log L|^{\hat{a}} f_{\chi} \left( L^2 t / (\log L)^{4/3} \right), \quad (\text{H10})$$

where we have used the MF values  $\nu = 1/2$  and  $\eta = 0$ . The logarithmic corrections have been computed making use of the renormalization group and their values are [42, 43, 47]:  $\hat{q} = 1/6$  and  $\hat{a} = 2/3$ .

### 2. Simulation results

We have carried out simulations for systems with size  $L$  ranging from  $L = 3$  to  $L = 9$  and for temperatures between  $T_{\min} = 3.012$  and  $T_{\max} = 3.031$ . The number of MCS used for each sample as well as the number of samples are reported in Table IV.

$L$	MCS	#Samples
3	409600	8500
4	409600	6500
5	409600	5500
6	409600	4000
7	409600	4000
8	204800	3000
9	307200	1000

TABLE IV. Table showing the number of samples (independent systems with different values of the interaction coupling  $J$ 's) simulated and the number of MCS made during each simulation for each value of the lattice size  $L$ .

The critical temperature have been computed by studying the Binder cumulant and the correlation length (see Fig. 9) and we have obtained a value of

$$T_c = 3.033(1), \quad (\text{H11})$$

which is compatible with the previous known results obtained via simulations  $T_c = 3.035(10)$  [36] and a high temperature expansion  $T_c = 3.027(5)$  [37].

The theoretical value of the critical exponents and logarithmic corrections can be checked using the collapse method, i.e. by representing  $\xi_2/L |\log L|^{1/6}$  and  $\chi_{SG}/L^{2-\eta} |\log L|^{2/3}$  vs  $L^{1/\nu} t / (\log L)^{4/3}$ . Since the expressions (H9) and (H10) holds asymptotically for large values of  $L$ , one would expect the curves for different lattice size to collapse into a single curve near the critical temperature when  $L \gg 1$  if and only if the theoretical values of  $\nu$ ,  $\eta$ ,  $\hat{q}$  and  $\hat{a}$  are the correct ones. The results can be checked in Fig. 10.

However, it is difficult to discern with precision the correct value of the logarithmic correction from Fig. 10. Alternatively, we can check  $\hat{q}$  and  $\hat{a}$  by representing  $\chi_{SG}(T_c)/L^2 (\log L)^{2/3}$  and  $\xi_2(T_c)/L (\log L)^{1/6}$  vs the lattice size  $L$ . If the scaling behaviour (H9) and (H10) holds, and the theoretical values of the critical exponents are compatible with our data, then we would observe a constant behaviour (represented by the blue line in Fig. 11).

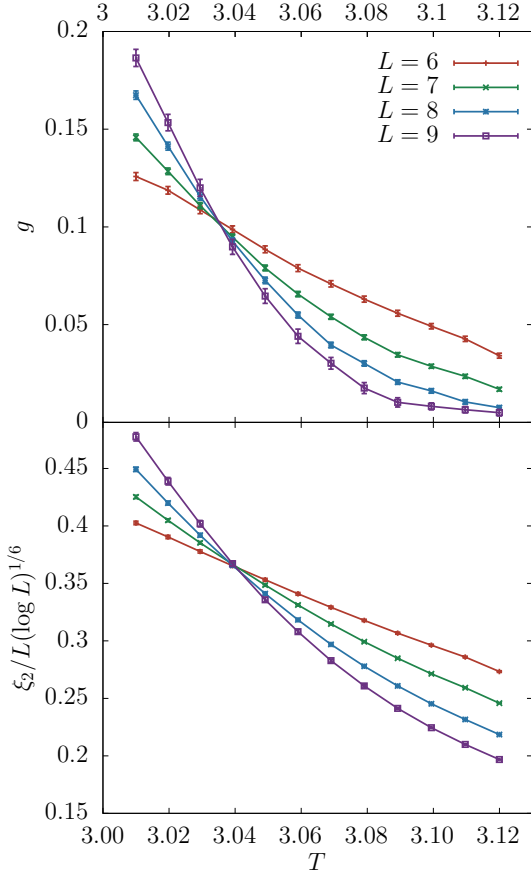


FIG. 9. Binder cumulant  $g$  (on the **top**), Eq. (H2), and the second moment correlation length  $\xi_2$  divided by the lattice size  $L$  and by the logarithmic correction term  $(\log L)^{1/6}$  (on the **bottom**) as a function of temperature for lattice sizes between  $L = 6$  and  $L = 9$ . The presence of an intersection between the curves at temperatures  $T_c^B$  and  $T_c^\xi$  signals the existence of a continuous phase transition.

From the analysis above, we conclude that our simulation results are compatible with the MF values of the critical exponents and with the theoretical values of the logarithmic corrections  $\hat{q} = 1/6$  and  $\hat{a} = 2/3$ .

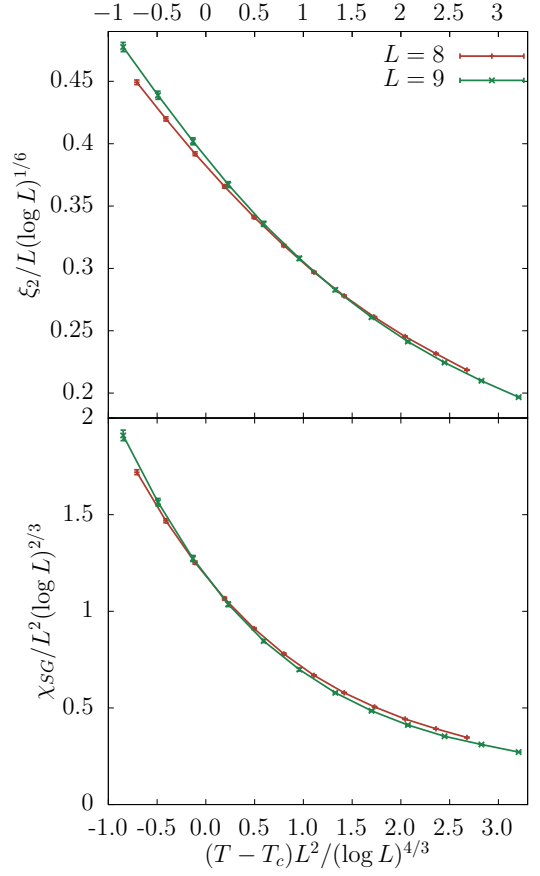


FIG. 10. Second moment correlation length  $\xi_2$  divided by the lattice size  $L$  and by the logarithmic correction term  $(\log L)^{1/6}$  (on the **top**) and the spin glass susceptibility  $\chi_{SG}$  divided by  $L^{2-\eta}$  (using the mean field result  $\eta = 0$ ) and by the logarithmic correction term  $(\log L)^{2/3}$  (on the **bottom**) as a function of the argument of the scaling functions  $f_\xi$  and  $f_\chi$  for lattice sizes  $L = 8$  and  $L = 9$ . Since Eqs. (H9) and (H10) hold asymptotically for large values of  $L$  we would expect the two curves to collapse into a single one only if the used values of the logarithmic correction critical exponents  $\hat{q}$  and  $\hat{a}$  are the correct one.

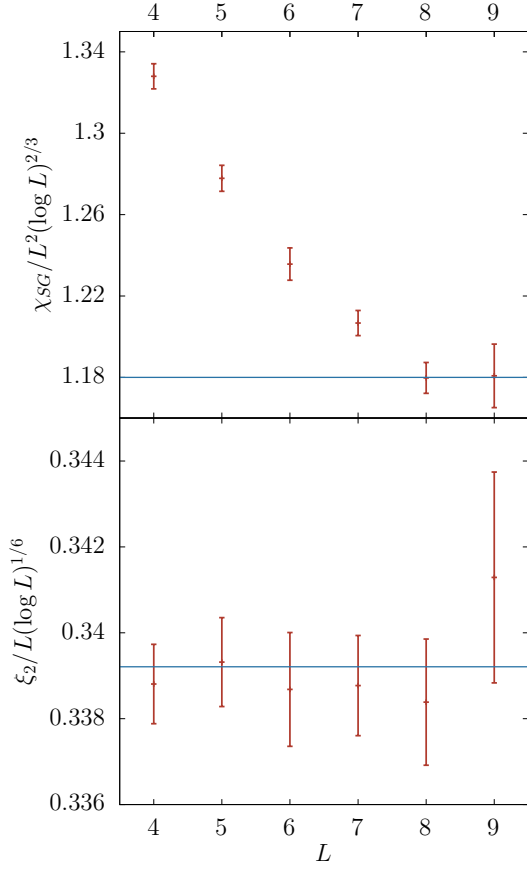


FIG. 11. Plot of  $\chi_{SG}(T_c)/L^2(\log L)^{2/3}$  (on the **top**) and  $\xi_2(T_c)/L(\log L)^{1/6}$  (on the **bottom**) versus the lattice size  $L$ . Our data approach asymptotically to a constant value for  $L \gg 1$ , from which we conclude that they are compatible with the values  $\hat{a} = 2/3$  and  $\hat{q} = 1/6$ . The constant behaviour for the bottom plot was expected since the scaling of  $\xi$  was used to determine the value of  $T_c$ .

- 
- [1] J. R. L. de Almeida and D. J. Thouless, Stability of the Sherrington-Kirkpatrick solution of a spin glass model, *J. Phys. A: Math. Gen.* **11**, 983 (1978).
- [2] G. Parisi, M. A. Virasoro, and M. Mézard, *Spin Glass Theory and Beyond* (World Scientific, 1987).
- [3] A. P. Young, *Spin Glasses and Random Fields* (World Scientific, 1998).
- [4] K. H. Fischer and J. A. Hertz, *Spin Glasses* (Cambridge University Press, 1991).
- [5] E. Bolthausen and A. Bovier, *Spin Glass* (Springer, 2007).
- [6] K. G. Wilson and J. Kogut, The renormalization group and the  $\epsilon$ -expansion, *Physics Reports* **12**, 75 (1974).
- [7] D. J. Amit and V. Martin-Mayor, *Field theory, the renormalization group, and critical phenomena: graphs to computers* (World Scientific, 2005).
- [8] A. B. Harris, T. C. Lubensky, and J.-H. Chen, Critical properties of spin-glasses, *Phys. Rev. Lett.* **36**, 415 (1976).
- [9] M. Baity-Jesi, R. A. Baños, A. Cruz, L. A. Fernandez, J. M. Gil-Narvion, A. Gordillo-Guerrero, D. Iniguez, A. Maiorano, F. Mantovani, E. Marinari, V. Martín-Mayor, J. Monforte-Garcia, A. Muñoz Sudupe, D. Navarro, G. Parisi, S. Perez-Gaviro, M. Pivanti, F. Ricci-Tersenghi, J. J. Ruiz-Lorenzo, S. F. Schifano, B. Seoane, A. Tarancon, R. Tripiccion, and D. Yllanes (Janus Collaboration), Critical parameters of the three-dimensional Ising spin glass, *Phys. Rev. B* **88**, 224416 (2013), arXiv:1310.2910.
- [10] A. J. Bray and S. A. Roberts, Renormalisation-group approach to the spin glass transition in finite magnetic fields, *J. Phys. C: Solid St. Phys.* **13**, 5405 (1980).
- [11] I. R. Pimentel, T. Temesvári, and C. De Dominicis, Spin-glass transition in a magnetic field: A renormalization group study, *Phys. Rev. B* **65**, 224420 (2002).
- [12] W. L. McMillan, *J. Phys. C: Solid State Phys.* **17**, 3179 (1984).
- [13] D. S. Fisher and D. A. Huse, Ordered phase of short-range ising spin-glasses, *Phys. Rev. Lett.* **56**, 1601 (1986).
- [14] A. J. Bray and M. A. Moore, Scaling theory of the ordered phase of spin glasses, in *Heidelberg Colloquium on Glassy Dynamics*, Lecture Notes in Physics No. 275, edited by J. L. van Hemmen and I. Morgenstern (Springer, Berlin, 1987).
- [15] D. S. Fisher and D. A. Huse, Nonequilibrium dynamics of spin glasses, *Phys. Rev. B* **38**, 373 (1988).
- [16] J. Yeo and M. A. Moore, Critical point scaling of ising spin glasses in a magnetic field, *Phys. Rev. B* **91**, 104432 (2015).
- [17] A. J. Bray and M. A. Moore, Disappearance of the de Almeida-Thouless line in six dimensions, *Phys. Rev. B* **83**, 224408 (2011), arXiv:1102.1675.
- [18] G. Parisi and T. Temesvári, Replica symmetry breaking in and around six dimensions, *Nucl. Phys. B* **858**, 293 (2012), arXiv:1111.3313.
- [19] R. R. P. Singh and A. P. Young, Critical and griffiths-mccoy singularities in quantum ising spin glasses on  $d$ -dimensional hypercubic lattices: A series expansion study, *Phys. Rev. E* **96**, 022139 (2017).
- [20] M. C. Angelini, C. Lucibello, G. Parisi, G. Perrupato, F. Ricci-Tersenghi, and T. Rizzo, *Phys. Rev. Lett.* **128**, 075702 (2022).
- [21] P. Charbonneau and S. Yaida, Nontrivial critical fixed point for replica-symmetry-breaking transitions, *Phys. Rev. Lett.* **118**, 215701 (2017).
- [22] P. Charbonneau, Y. Hu, A. Raju, J. P. Sethna, and S. Yaida, Morphology of renormalization-group flow for the de almeida-thouless-gardner universality class, *Phys. Rev. E* **99**, 022132 (2019).
- [23] J. Höller and N. Read, One-step replica-symmetry-breaking phase below the de almeida-thouless line in low-dimensional spin glasses, *Phys. Rev. E* **101**, 042114 (2020).
- [24] L. A. Fernandez, I. Gonzalez-Adalid Pemartin, V. Martín-Mayor, G. Parisi, F. Ricci-Tersenghi, T. Rizzo, J. J. Ruiz-Lorenzo, and M. Veca, Numerical test of the replica-symmetric hamiltonian for correlations of the critical state of spin glasses in a field, *Phys. Rev. E* **105**, 054106 (2022).
- [25] R. A. Baños, A. Cruz, L. A. Fernandez, J. M. Gil-Narvion, A. Gordillo-Guerrero, M. Guidetti, D. Iniguez, A. Maiorano, E. Marinari, V. Martín-Mayor, J. Monforte-Garcia, A. Muñoz Sudupe, D. Navarro, G. Parisi, S. Perez-Gaviro, J. J. Ruiz-Lorenzo, S. F. Schifano, B. Seoane, A. Tarancon, P. Tellez, R. Tripiccion, and D. Yllanes, Thermodynamic glass transition in a spin glass without time-reversal symmetry, *Proc. Natl. Acad. Sci. USA* **109**, 6452 (2012).
- [26] M. Baity-Jesi, R. A. Baños, A. Cruz, L. A. Fernandez, J. M. Gil-Narvion, A. Gordillo-Guerrero, D. Iniguez, A. Maiorano, M. F., E. Marinari, V. Martín-Mayor, J. Monforte-Garcia, A. Muñoz Sudupe, D. Navarro, G. Parisi, S. Perez-Gaviro, M. Pivanti, F. Ricci-Tersenghi, J. J. Ruiz-Lorenzo, S. F. Schifano, B. Seoane, A. Tarancon, R. Tripiccion, and D. Yllanes, Dynamical Transition in the  $D=3$  Edwards-Anderson spin glass in an external magnetic field, *Phys. Rev. E* **89**, 032140 (2014), arXiv:1307.4998.
- [27] M. Baity-Jesi, R. A. Baños, A. Cruz, L. A. Fernandez, J. M. Gil-Narvion, A. Gordillo-Guerrero, D. Iniguez, A. Maiorano, M. F., E. Marinari, V. Martín-Mayor, J. Monforte-Garcia, A. Muñoz Sudupe, D. Navarro, G. Parisi, S. Perez-Gaviro, M. Pivanti, F. Ricci-Tersenghi, J. J. Ruiz-Lorenzo, S. F. Schifano, B. Seoane, A. Tarancon, R. Tripiccion, and D. Yllanes, The three dimensional Ising spin glass in an external magnetic field: the role of the silent majority, *J. Stat. Mech.* **2014**, P05014 (2014), arXiv:1403.2622.
- [28] L. A. Fernandez, V. Martín-Mayor, S. Perez-Gaviro, A. Tarancon, and A. P. Young, Phase transition in the three dimensional Heisenberg spin glass: Finite-size scaling analysis, *Phys. Rev. B* **80**, 024422 (2009).
- [29] G. Parisi and T. Rizzo, Critical dynamics in glassy systems, *Phys. Rev. E* **87**, 012101 (2013).
- [30] In Ref. [24] the four-dimensional Ising spin glass in a field was analyzed numerically but  $\omega_1$  and  $\omega_2$  were computed only from three- and four- replica estimators.
- [31] L. Leuzzi, G. Parisi, F. Ricci-Tersenghi, and J. J. Ruiz-Lorenzo, Ising spin-glass transition in a magnetic field outside the limit of validity of mean-field theory, *Phys. Rev. Lett.* **103**, 267201 (2009), arXiv:0811.3435.
- [32] K. Hukushima and K. Nemoto, Exchange Monte Carlo

- method and application to spin glass simulations, J. Phys. Soc. Japan **65**, 1604 (1996), arXiv:cond-mat/9512035.
- [33] E. Marinari, Optimized Monte Carlo methods, in *Advances in Computer Simulation*, edited by J. Kerstész and I. Kondor (Springer-Verlag, 1998).
- [34] A. Billoire, L. A. Fernandez, A. Maiorano, E. Marinari, V. Martin-Mayor, J. Moreno-Gordo, G. Parisi, F. Ricci-Tersenghi, and J. J. Ruiz-Lorenzo, Dynamic variational study of chaos: spin glasses in three dimensions, Journal of Statistical Mechanics: Theory and Experiment **2018**, 033302 (2018).
- [35] One can compare this factor with the values of  $\chi_R/\chi_A$  at  $T_c(h=0)$ , which are  $\chi_R/\chi_A \simeq 1.35, 1.65, 1.85, 1.96$  for  $L=5, 6, 7$  and  $8$  respectively.
- [36] J. Wang and A. P. Young, Monte carlo study of the six-dimensional ising spin glass, Journal of Physics A: Mathematical and General **26**, 1063 (1993).
- [37] L. Klein, J. Adler, A. Aharony, A. B. Harris, and Y. Meir, Series expansions for the ising spin glass in general dimension, Phys. Rev. B **43**, 11249 (1991).
- [38] M. Nightingale, Scaling theory and finite systems, Physica A: Statistical Mechanics and its Applications **83**, 561 (1976).
- [39] H. G. Ballesteros, L. A. Fernandez, V. Martín-Mayor, and A. Muñoz Sudupe, Phys. Lett. B **387**, 125 (1996).
- [40] H. G. Ballesteros, L. A. Fernandez, V. Martín-Mayor, and A. Muñoz Sudupe, Nucl. Phys. B **483**, 707 (1997).
- [41] Considering only leading corrections to scaling, the quotient of  $\partial R_{12}/\partial T$  at the crossing point for  $(L_1, L_2)$  is  $Q = (L_2/L_1)^{1/\nu}[1 + A_1 L_2^{-\omega}]/[1 + A_1 L_1^{-\omega}]$ , where  $A_1$  is an amplitude and  $\omega$  is the leading corrections-to-scaling exponent. If  $L_2 = L_1 + 1$ ,  $Q = (L_2/L_1)^{1/\nu}[1 + A_1(L_2^{-\omega} - L_1^{-\omega}) + \dots]$ . Thus, the exponents we are computing from the fits are  $\omega_{\nu,\eta} = \omega + 1$ .
- [42] J. J. Ruiz-Lorenzo, Logarithmic corrections for spin glasses, percolation and lee-yang singularities in six dimensions, Journal of Physics A: Mathematical and General **31**, 8773 (1998).
- [43] J. J. R. Lorenzo, Revisiting (logarithmic) scaling relations using renormalization group, Condensed Matter Physics **20**, 13601: 1–10 (2017).
- [44] P. Young, *Everything you wanted to know about Data Analysis and Fitting but were afraid to ask* (Springer Cham, 2015).
- [45] B. Efron, *The jackknife, the bootstrap, and other resampling plans*, Vol. 38 (Siam, 1982).
- [46] <https://www.intel.com/content/www/us/en/docs/intrinsics-guide/index.html>.
- [47] R. Kenna, D. A. Johnston, and W. Janke, Scaling relations for logarithmic corrections, Phys. Rev. Lett. **96**, 115701 (2006).